



# Deposition and characterisation of vanadium oxide thin films: Linking single crystal and supported catalyst

H. Poelman<sup>a,\*</sup>, G. Silversmit<sup>a,1</sup>, D. Poelman<sup>a</sup>, G.B. Marin<sup>b</sup>, B.S. Sels<sup>c</sup>

<sup>a</sup> Ghent University, Surface Physics and Thin Films Division, Department of Solid State Sciences, Krijgslaan 281, S1, B-9000 Gent, Belgium

<sup>b</sup> Ghent University, Laboratorium voor Chemische Technologie, Department of Chemical Engineering, Krijgslaan 281, S5, B-9000 Gent, Belgium

<sup>c</sup> K.U. Leuven, Department of Molecular and Microbiological Systems, Kasteelpark Arenberg 23, B-3001 Heverlee, Belgium

## ARTICLE INFO

### Article history:

Available online 28 October 2008

### Keywords:

Vanadium oxide  
Thin films  
Sputter deposition  
Titania supported vanadia  
Model catalysts  
ODH

## ABSTRACT

Thin films can make a useful link between single crystal and supported vanadium oxide. The deposition of vanadium oxide thin films with physical vapour deposition techniques ensures clean and highly controllable synthesis. The resulting material is easily accessed with surface sensitive techniques. On flat TiO<sub>2</sub> anatase substrates, XPS–XPD and UPS indicated that the vanadia deposition was epitaxial, and fully oxidised if performed *in situ*. A step closer to typical industrial catalysts was achieved by sputter deposition onto sub-millimetre inert particles. In addition to surface characterisation, these model particle catalysts allow use in reactors for catalytic testing under relevant process conditions. On both silica and titania supports, sputter deposited vanadia of varying thickness proved to be equally well dispersed. Oxidative dehydrogenation (ODH) activity was higher over vanadia/titania (anatase) than over vanadia/silica, demonstrating the synergetic interaction between anatase and vanadia. Highest activity in alkane ODH was observed for vanadia a few monolayers thick, supported on titania-coated particles.

© 2008 Elsevier B.V. All rights reserved.

## 1. Introduction

Vanadium pentoxide (V<sub>2</sub>O<sub>5</sub>) has a long history as research subject. Its single crystal structure was determined in 1961 by Bachmann, Ahmed and Barnes [1]. Large single crystals with high purity can be successfully grown, e.g. by means of the molten zone technique [2]. Since then, the single crystal material has been characterised in many ways: electron energy loss spectroscopy ((HR)EELS) [3] for surface vibrational properties, microscopic techniques (e.g. STM, TEM) [4], low energy electron diffraction (LEED) for surface crystallography [5], atomic force microscopy (AFM) for topology [6], X-ray photoelectron spectroscopy (XPS) [7,8], etc.

Vanadium pentoxide plays a very important role in heterogeneous catalysis. Catalysts based on V<sub>2</sub>O<sub>5</sub> are used in several industrial reactions such as total oxidation (e.g. SO<sub>2</sub> to SO<sub>3</sub>), partial oxidation (e.g. *o*-xylene to phthalic anhydride) and selective reduction reactions (selective catalytic reduction, SCR, e.g. elimination of NO<sub>x</sub> with NH<sub>3</sub>) [9]. In most cases, V<sub>2</sub>O<sub>5</sub>-based

catalysts consist of a vanadia phase deposited onto a porous oxide support, like Al<sub>2</sub>O<sub>3</sub>, SiO<sub>2</sub>, TiO<sub>2</sub>, etc. Supported vanadia in general exhibits better catalytic properties than unsupported vanadia. The support assures mechanical strength and provides a large surface area of the active phase. The latter function was long considered the major reason for the superior behaviour of supported vanadia as the support was thought to be inert in the catalytic process [9]. However, it was found later that activity and selectivity of the vanadia strongly depend upon the nature of the oxide support [10], in short termed the ‘support effect’. In this respect, titania in the anatase phase occupies a privileged position as it strongly enhances the catalytic activity of vanadia for several reactions [11].

For a given weight of material, the most obvious difference between supported catalysts and single crystals is the available active surface area. For a single crystal, the specific surface area (i.e. the surface area per weight) is essentially determined by the outer crystal planes, sometimes slightly increased by surface roughness. The mere decrease of particle size from millimetre down to micron or nanometre scale, yields an important increase in specific surface area. The latter is determined using the Brunauer–Emmett–Teller (BET) method based on the physical adsorption of gas molecules on a solid [12]. With a detection limit of typically 0.1 m<sup>2</sup>/g, this technique is solely of use for particle material. The increased area presents more sites available for adsorption and reaction, hence a gain in activity per weight. The same still holds if the active

\* Corresponding author. Tel.: +32 9 264 43 71; fax: +32 9 264 49 96.

E-mail address: [hilde.poelman@UGent.be](mailto:hilde.poelman@UGent.be) (H. Poelman).

<sup>1</sup> Present address: Ghent University, X-ray Microspectroscopy and Imaging Research Group (XMI), Department of Analytical Chemistry, Krijgslaan 281, S12, B-9000 Gent, Belgium.

material is applied on a suitable support, as in the case of supported vanadia.

The (particle) size difference between single crystals and supported catalysts is responsible for a shift in techniques applicable for investigation. While measurements like XPS remain applicable, surface techniques such as LEED, EELS, AFM are of less or no use on supported samples. On the other hand, new tools become accessible: Temperature Programmed Reduction (TPR), Diffuse Reflection Spectroscopy (DRS), Raman Spectroscopy, etc. However, the most striking advantage of supported catalysts over single crystalline material is the more straightforward activity determination at reaction conditions in terms of conversion ( $X$ ), turnover frequency (TOF) and/or selectivity ( $S$ ). Combining these catalytic properties with the physicochemical ones determined with the above mentioned methods eventually allows to investigate the structure–activity relationships of the specific catalyst system.

The scale difference between single crystals and supported catalysts can be bridged by the use of thin films of vanadium oxide. Under appropriate conditions, films can be deposited as a stoichiometric and crystalline phase. Such films are well defined and allow the use of surface sensitive techniques to access the physicochemical properties. With a special setup, thin films can equally be applied on small supports, allowing investigation of catalytic properties.

## 2. Thin film deposition

Several techniques are available for thin film deposition. Most popular among the chemical methods is Chemical Vapour Deposition (CVD) where a film is generated by reaction of appropriate precursors at the substrate surface [13]. The deposition can be stimulated by supplying extra energy during the process, e.g. by means of plasma enhancement (PECVD) or laser stimulation (LCVD). A special form of this technique is Atomic Layer Deposition (ALD) [14], which splits the CVD reaction process at the surface into two parts. A first precursor pulse covers the available substrate surface. Upon the second precursor pulse, reaction occurs with the adsorbed species of the previous pulse, yielding a dense and uniform single layer coating. By means of sequential pulsing of the two precursors, highly controllable layer-by-layer growth is achieved at nanometre scale. Wet chemical synthesis of vanadium oxide films is another route for thin film deposition and involves spin or dip coating or drop casting of a solution or gel followed by suitable drying [15].

With physical vapour deposition (PVD) precisely controlled and very clean vanadia films can be deposited. This is due to the use of a (high) vacuum environment and of high purity source materials, which allows a higher film purity, compared to non-vacuum-based techniques. The desired material is brought into the gas-phase from where it travels to the substrate support. This gas-phase state can be obtained through thermal or electron beam evaporation [16], from which Molecular Beam Epitaxy (MBE) is derived [17], pulsed laser deposition (PLD) [18] or sputter deposition [19]. In order to obtain vanadium oxide, one can either start from elemental source material V or from a compound source. Stoichiometric vanadium oxide is then obtained either by depositing reactively, i.e. by adding oxygen to the atmosphere so that the vaporized or sputtered elements react at the substrate or target surface to form the required oxide, or by performing a post-deposition annealing in oxygen or air. To achieve a certain degree of crystallinity in the film, extra energy input is often required to stimulate surface diffusion. This can be done in the form of substrate heating, post-deposition annealing or ion bombardment of the film during deposition (IBAD: ion beam

assisted deposition). The latter allows to modify the film morphology or form different phases.

Sputter deposition is a well-established technique for the production of thin films of  $V_2O_5$ . The technique is based on the impact of plasma ions on a target, from which material is knocked out and deposited onto a support [20]. It requires the addition of oxygen as reactive gas to the sputter plasma in order to obtain fully oxidised layers, even when  $V_2O_5$  is used as target material. When magnets are added to the back of the target the ionisation in the plasma is enhanced, yielding a more efficient sputter process (i.e.: magnetron sputtering) (Fig. 1). To date, this technique is used most frequently for coating flat substrates. However, in combination with a rotating container, it can equally serve to coat particle-like supports [21]. For this purpose, the vacuum chamber is equipped with a rotating drum inside which sputter devices are mounted. During deposition, the drum rotation makes the particles tumble, so that all sides are exposed to the sputter flux (Fig. 2). Both plane and rotatable targets can be used, the latter assuring a more efficient consumption of the target material.

When vanadium oxide is deposited on suitable titania supports, model systems can be created that link the advantages of surface analytical techniques and of supported catalyst characterisation. A first type of  $V_2O_5/TiO_2$  film system, named crystalline model system, consists of a crystalline thin film on a single crystal substrate. As anatase is a favourite support in heterogeneous catalysis, such model requires a single crystal anatase substrate. However, such crystals are hard to grow as the stable phase of  $TiO_2$  at room temperature is rutile rather than anatase. Successful attempts were made using chemical transport methods [22] yielding millimetre-size anatase crystals. As an alternative, one can use anatase minerals, which can be oriented, sawn and polished to yield the desired crystal plane. Another option is to start from anatase thin films, grown epitaxially onto a suitable substrate, e.g.  $LaAlO_3$  [23,24]. Different preferential orientations of the anatase films can thus be obtained. In this work, thin films were deposited on mineral anatase slices to yield a flat  $V_2O_5/TiO_2(001)$  anatase model system.

A second approach to model supported vanadia, is the use of coated particles. Thin films of vanadia are then applied onto non-porous inert particles in a dedicated sputter drum. Apart from the film–support interaction, the properties of these sputter deposited catalysts are only determined by the specific sputter conditions, which are highly reproducible. Hence, they can be referred to as model catalysts and examined by physical and chemical means. Moreover, by consecutive sputter deposition from different targets, several layer combinations can be synthesised. As such, sequential depositions of titania and vanadia were performed, resulting in supported  $VO_x/TiO_2$  particle model catalysts.

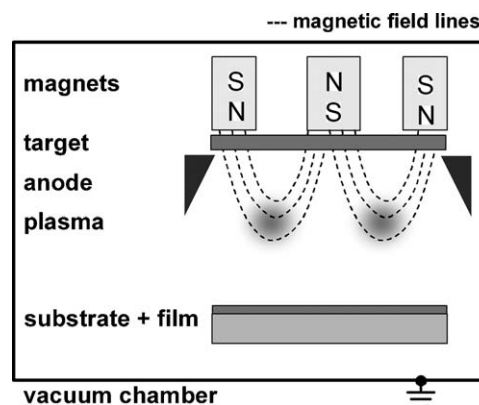
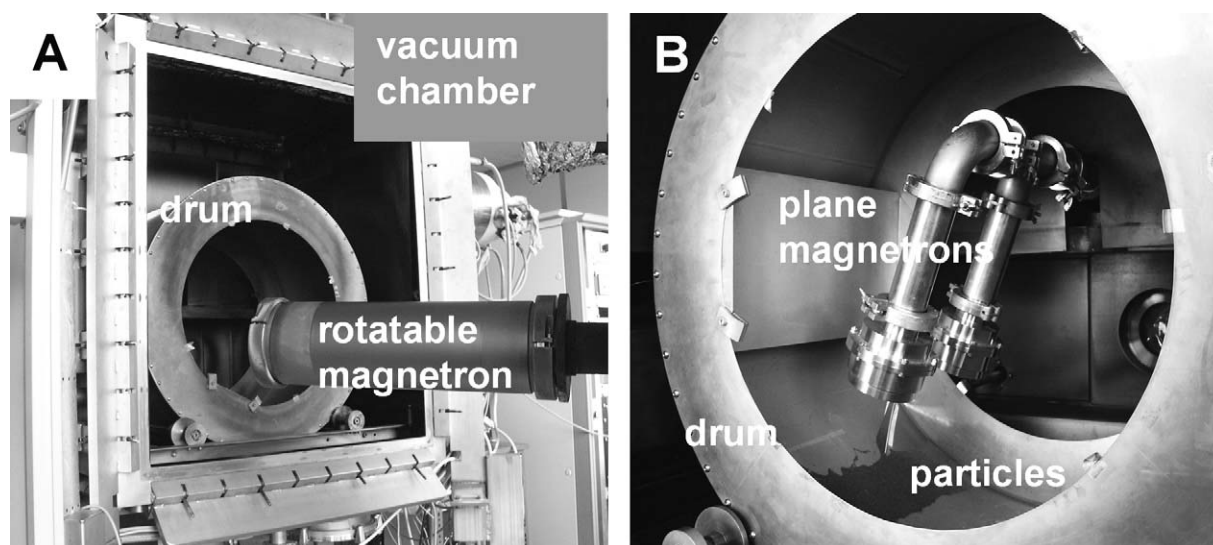


Fig. 1. Schematic view of a setup for magnetron sputter deposition.



**Fig. 2.** Vacuum chamber with rotating drum for the coating of particle supports: (A) open chamber with drum and rotatable cylindrical magnetron; (B) drum with particles and two plane circular magnetrons.

This paper highlights results obtained on thin film vanadia systems, both on flat and particle supports, demonstrating the possibilities of combining surface analytical tools with catalytic testing on such model systems.

### 3. Experimental: deposition and characterisation

#### 3.1. Flat $V_2O_5/TiO_2(001)$ anatase model system

The crystalline model systems were produced starting from (001)-oriented slices of mineral anatase. After introduction in the UHV chamber, the anatase surface was cleaned by alternating  $Ar^+$  bombardment ( $\sim 1 \times 10^{-2}$  Pa, 300–500 eV,  $\sim 1.5 \mu A$ ) and annealing in  $O_2$  (200–350 °C,  $\sim 1 \times 10^{-1}$  Pa) until a bright LEED pattern was observed.

Vanadia thin films were applied using reactive DC magnetron sputtering from a plane circular magnetron. A polycrystalline  $V_2O_5$  sputter target was used, obtained by melting  $V_2O_5$  powder in a crucible. By quenching the melt, fast needle-like growth occurred. The deposition was performed under 0.1–1.0 Pa  $O_2$ , with a power of  $\sim 10 W/cm^2$  and a rate of about 0.3 nm/min. First model systems were prepared in the preparation chamber of a high resolution electron energy loss (HREELS) spectrometer (SEDRA, ISA Riber, France). The layer formation was monitored using LEED and HREELS (primary electron energy  $E = 12$  eV, energy resolution FWHM = 5 meV). A model system with an estimated vanadia thickness of 0.3 nm, i.e.  $\sim 1$  monolayer, was further examined ex situ with X-ray photoelectron diffraction (XPD). This technique gives information about short-range order around an element. It is based on the increase of intensity of an emitted photoelectron wave along internuclear emitter–scatterer axes, due to interference effects [25]. Measurements were performed ex situ in an ultra high vacuum (UHV) PerkinElmer Phi 5500 system, allowing polar and azimuthal rotation of the sample with a  $1^\circ$  angular resolution. X-ray photoelectron diffraction ( $h\nu = 1486.6$  eV) intensity scans were recorded by measuring the  $Ti2p_{3/2}$ ,  $O1s$  and  $V2p_{3/2}$  photoline areas at a  $28^\circ$  polar angle with respect to the surface, with a  $2^\circ$  azimuthal step. For this polar angle strong scattering is expected to occur along the anatase  $a$ - and  $b$ -axes [26], allowing easy identification of the anatase major axes in an azimuthal  $Ti2p$  pattern.

In situ UPS measurements were performed at the SA73 beamline of the S.ACO storage ring at the LURE laboratory (Orsay,

France). Here, vanadia depositions were performed on a clean anatase (001) slice in an UHV attachment to the preparation chamber. By consecutive depositions, the thickness of the vanadia film was increased stepwise with 0.2 nm at each deposition, allowing intermediate measurements. After each cycle, UPS measurements were obtained with an excitation energy of 150 eV and  $V3p$ ,  $Ti3p$ ,  $O2s$  and valence band (VB) spectra were recorded with 0.2–0.3 eV energy resolution.

#### 3.2. Supported $VO_x/TiO_2$ particle model catalysts

In the dedicated sputter drum, supported vanadium oxide catalysts were synthesized by sputter deposition onto non-porous inert spherical beads (ZIR337, Phibo Industries, 67 wt%  $ZrO_2$ –33 wt%  $SiO_2$ , 250–425  $\mu m$  diameter). Vanadia was sputter deposited either on bare beads, presenting a silica surface (denoted Si), or on beads coated previously with a  $\sim 20$  nm thick titania film, to yield a titania support (denoted Ti). By varying the deposition time, the thickness of the vanadia film was adjusted, ranging from well below the monolayer up to several monolayers. An extra anneal treatment in air was applied to improve crystallinity and stoichiometry. Details of the synthesis procedure are described elsewhere [21]. Particle catalysts are labelled according to the support, Ti or Si, and the vanadia thin film with its deposition time in minutes, e.g.  $TiV60$  denotes a catalyst consisting of a  $TiO_2$  coated support (Ti) and a 60 min  $V_2O_5$  thin film.

The morphology of the sample with thickest depositions  $TiV330$  was visualised using Atomic Force Microscopy in non-contact mode (AFM; Topometrix TMX 2010) and bright field transmission electron microscopy (TEM; JEOL 3000F FEG electron microscope, 300 kV, 0.2 nm point resolution).

XPS was performed in a PerkinElmer PHI ESCA 5500 system with monochromatic  $Al K\alpha$  source. In view of the bead size and shape, a wide detection mode was chosen to cover several beads. The base pressure of the XPS analysis chamber was below  $1 \times 10^{-7}$  Pa. Experiments were performed with 220 W source power and an acceptance angle of  $\pm 7^\circ$ . The analyser axis made an angle of  $45^\circ$  with the sample surface.  $Si2p$ ,  $Zr3d$ ,  $C1s$ ,  $Ti2p$ ,  $O1s$  and  $V2p$  core levels were measured in high-resolution mode (pass energy 58.70 eV, step 0.13 eV).  $O1s$  and  $V2p$  signals were collected in one energy window. For the kinetic energies of  $V2p$  and  $Ti2p$  in their

respective oxides,  $V_2O_5$  and  $TiO_2$ , the XPS information depth amounts to 5–6 nm.

Eventually, the catalytic activity of the model particles was tested for propane and isobutane oxidative dehydrogenation (ODH). Steady state experiments were performed in a continuous flow reactor equipped with four parallel fixed-bed micro-reactors. The catalyst (1 g for  $C_3H_8$  and 0.5 g for  $iC_4H_{10}$ , without dissolution) was pre-treated for 3 h at 873 K in a gas flow containing He ( $12 \text{ ml min}^{-1}$ ) and  $O_2$  ( $3 \text{ ml min}^{-1}$ ). For the reaction, a feed of mixed He,  $C_3H_8$  (or  $iC_4H_{10}$ ) and  $O_2$  was used. Details of the reagent concentrations and flows are summarized in the caption of Fig. 11. Feed and products were analyzed with an on-line HP 5890 series II gas chromatograph. In the case of  $C_3H_8$ , the latter was equipped with two parallel poraplot Q columns, one connected to a FID and the other one to a TCD; for the product analysis in the  $iC_4H_{10}$  reactions, a poraplot Q column with FID detector was combined with a Molecular Sieve 5A column connected to a TCD. The reaction temperature was kept constant at 823 K for 300 min.

## 4. Results and discussion

### 4.1. Vanadium oxide thin films on flat substrates

Flat  $V_2O_5/TiO_2(001)$  anatase model systems were studied *ex situ* by means of XPS–XPD. Although the anatase substrate presented a bright (001) LEED image, no long range order was present after deposition of the vanadium oxide thin film. Despite the absence of long range order, XPD measurements were possible as these rely on local order around a specific element. Fig. 3 shows the XPD patterns of V2p, Ti2p and O1s for a fresh model catalyst with an estimated thickness of 1 monolayer. The  $90^\circ$  periodicity, along the major crystallographic axes of the  $TiO_2$  lattice, is reproduced by all curves, in particular by the V2p pattern from the top vanadia layer. The coincidence of major diffraction peaks indicates that the vanadium oxide monolayer presents the same orientation as the  $TiO_2$  anatase substrate, pointing towards epitaxial deposition with short-range order [27]. This result can serve as starting point for XPD simulations [28] or for periodic DFT calculations [29] to model the vanadia thin film structure on anatase.

To follow the growth of the thin film, sequential depositions of vanadia on anatase were followed by means of *in situ* techniques. Electron energy loss spectra taken in between depositions showed a gradual transition of the anatase loss spectrum towards the one of  $V_2O_5(001)$  (Fig. 4). In particular, the rise of the characteristic  $V=O$  vanadyl stretch vibration at 129 meV with respect

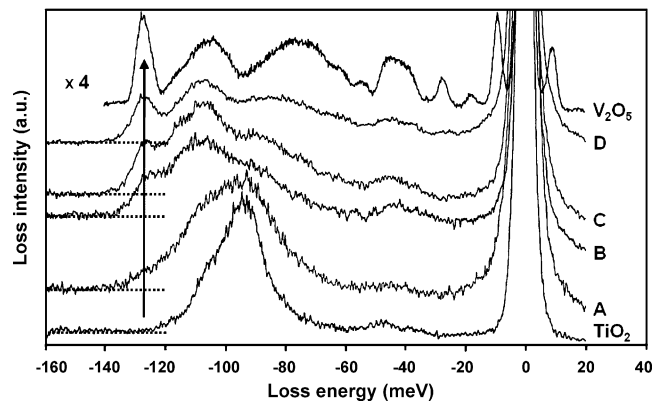


Fig. 4. Electron energy loss spectra (primary energy = 12 eV; FWHM = 5 meV) corresponding to consecutive sputter deposition cycles of vanadia on  $TiO_2(001)$  anatase; Bottom: spectrum for clean anatase (001) substrate; Top: enlarged reference spectrum from  $V_2O_5(001)$ ; Intermediate spectra: sputter deposited vanadia layers on anatase substrate with increasing vanadia estimated thickness. A: 1.5 nm, B: 7 nm, C: 13 nm, D: 20 nm. The arrow indicates the position of the characteristic  $V=O$  stretch vibration at 129 meV [34].

to the background line indicates that a vanadium oxide layer of increasing thickness has been deposited [30].

When model systems are synthesized in one UHV equipment and transferred through air to *ex situ* analysis equipment, contamination occurs which can easily lead to reduction of the layer, especially upon irradiation (i.e. photoreduction). In this way, a considerable amount (up to 40%) of  $V^{4+}$  can be found upon line shape analysis of V2p photolines from  $V_2O_5/TiO_2(001)$  anatase model systems [31]. To exclude air transfer contamination,  $V_2O_5/TiO_2(001)$  anatase model systems were also prepared and studied *in situ* by means of synchrotron UPS. A 0.5 ML (monolayer) stepwise deposition of  $V_2O_5$  provided a deeper insight into the thin film properties. In the V3p–Ti3p region, a gradual change was observed upon increasing film thickness (Fig. 5). Already with the first vanadia deposition, the work function of the anatase substrate was changed, noticeable as shift in peak positions to lower binding energy values. The V3p line evolved around 42 eV with each further deposition, while Ti3p (binding energy,  $E_b \sim 36.3$  eV) was

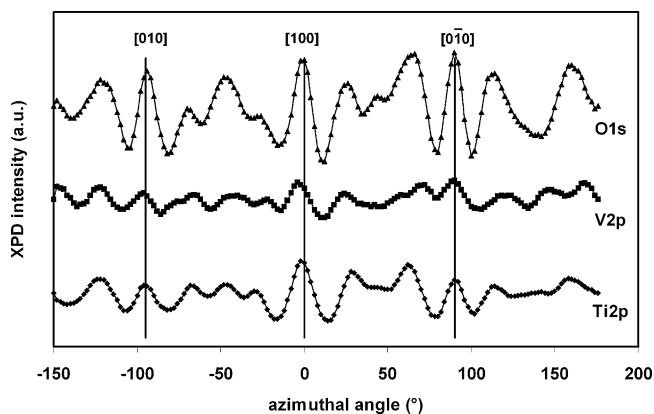


Fig. 3. experimental XPD patterns for O1s, Ti2p and V2p at  $28^\circ$  polar angle for a freshly prepared  $V_2O_5/TiO_2(001)$  anatase model catalyst (estimated thickness: close to 1 monolayer).

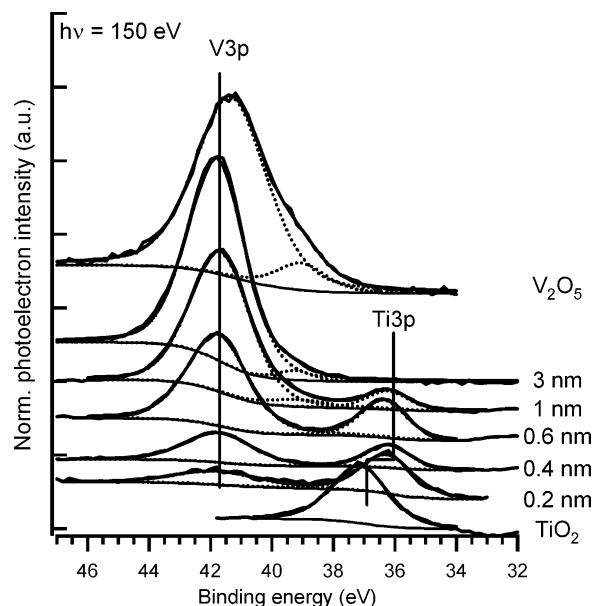


Fig. 5. UPS measurement of the V3p–Ti3p region for increasing thickness of vanadia on anatase.



gradually suppressed. Although all of the depositions and measurements were performed in situ in UHV, a weak multiplet structure was observed in the V3p photoline and a small 3d peak developed next to the valence band (not shown). These effects are due to a slight photoreduction of the deposited layers, caused by the photon irradiation and resulting in the presence of 3d electrons, typical for non-stoichiometric  $V_2O_5$  [32]. Fig. 6 shows how the 3d peak in the valence band region is non-existent in the firstly recorded single spectrum on a 1.6 nm  $V_2O_5/TiO_2$ , but emerging and growing in later spectra, following an increasing photon irradiation time of the sample [33].

The deposition of thin vanadia films on flat substrates opens new pathways of investigation regarding the structure and composition of the deposited film. Care has to be taken that upon production or analysis, the film does not suffer from reduction. However, given the low surface area of a film, it can never be used in a number of catalytic characterisation techniques or a true reaction setup. In order to get closer to industrial supported catalysts, one extra step has to be made, i.e. increasing the surface area by reducing the substrate particle size.

#### 4.2. Vanadium oxide thin films on particles

With the rotating drum (Fig. 2), vanadium oxide thin films were deposited with varying thickness on inert particles, either bare or titania coated. From XRD, titania was found to be polycrystalline anatase, while the vanadia remained XRD amorphous. By varying the sputter time between 5 and 330 min, the amounts of deposited vanadia were easily tuned from below the monolayer (ML) up to several ML.

On the longest deposition, TiV330, an image of the film surface was made on the micrometre scale with AFM in contact mode and compared to the surface of an uncoated particle (Fig. 7B and A resp.). The double deposition appears as a rough coating compared to the bare particle surface. In the nano-range, a TEM image showed the double deposition of titania and vanadia as one faint thin line (Fig. 8).

With increasing vanadia deposition time, ex situ XPS measurements showed essentially an increase of the relative V concentration, gradually covering the underlying titania material. The evolution of the atomic concentrations for O, V and Ti with deposition time is displayed in Fig. 9. Note that for the given kinetic energies of the photoelectrons V2p and Ti2p, the XPS information depth amounts to several atomic layers, which explains why Ti is measured even for the thickest vanadia deposition TiV330.

A remarkable result was found upon evaluation of the dispersion of the vanadia over the bare or titania-coated particles [34]. It turned out that this method of thin film synthesis on particles yielded vanadia coatings with similar dispersion on titania and silica (Fig. 10). This is especially peculiar for silica, since

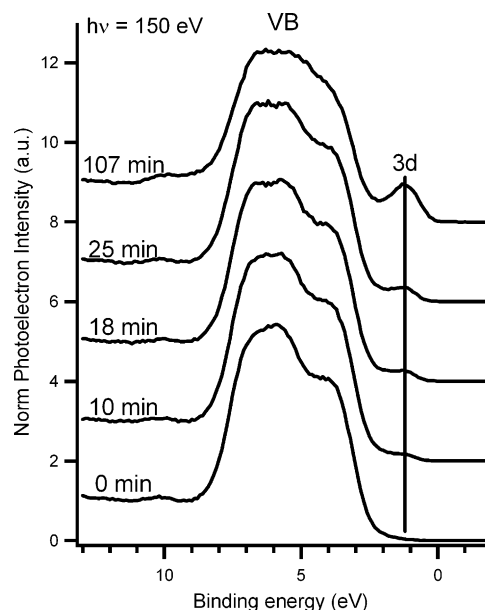


Fig. 6. Consecutive single scans and final multiple scan of the valence band for a 1.6 nm  $V_2O_5/TiO_2$  sample, with increasing photon irradiation time. Times indicated are the total irradiation times at the start of each single scan. The upper spectrum is the multiple spectrum of the valence band.

this support is thought to cause clustering of vanadia already from low coverage [35]. In classical wet synthesis, this clustering effect is related to pH influences. However, in our synthesis method using physical vapour deposition, the structural effect of the support material does not seem to affect the vanadia dispersion, or the speciation. Indeed, further analysis of the coated particles revealed that also the speciation and degree of polymerisation of vanadia were very similar for both types of supports: from isolated vanadates over polymeric species to strongly polymerized and crystalline  $V_2O_5$  for the highest vanadia loadings. An extensive investigation of the properties of these sputter coated particles can be found elsewhere [34].

The fact that dispersion, speciation and degree of polymerisation of the model particles are similar on both supports, means that any difference in activity should be ascribed to a structural or electronic influence of the support. This decoupling of speciation and activity from the support material is uniquely due to the synthesis by means of sputter deposition. Fig. 11 shows how the propane and isobutane conversion at 823 K vary with vanadia surface density over both supports. Conversions are low over all catalysts, due to the low amount of vanadia present in the reactor [34]. For both molecules, ODH conversion is higher for TiV particles, i.e. vanadia supported on anatase coated particles, than

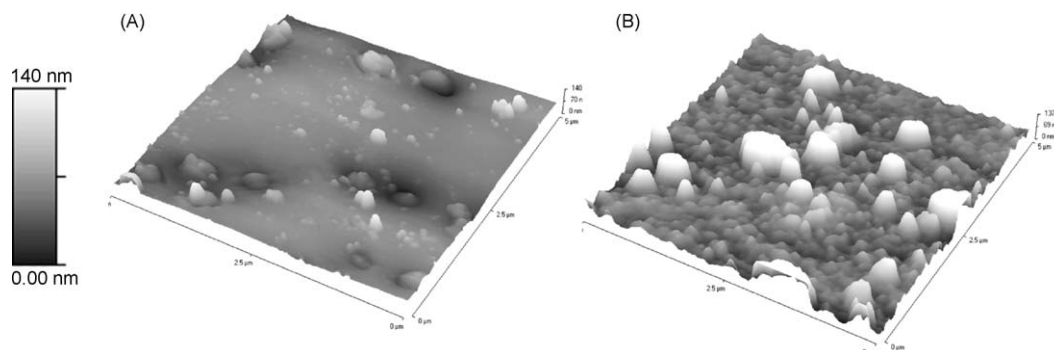
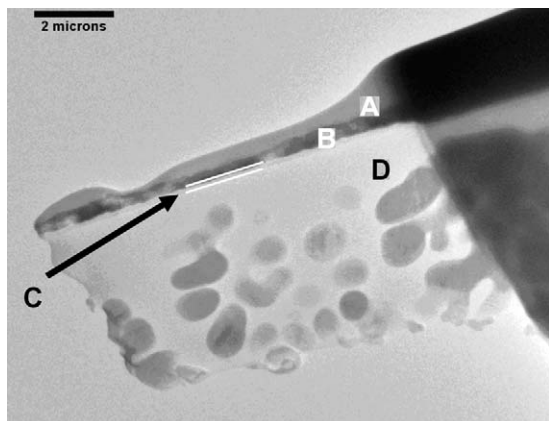


Fig. 7. AFM measurements in contact mode over a  $5 \mu m \times 5 \mu m$  area of the particle catalyst: (A) bare particle, (B) doubly coated TiV330.



**Fig. 8.** Bright field TEM image of TiV330, prepared by FIB. (A) Platinum protective layer, (B) gold protective layer, (C)  $\text{TiO}_2 + \text{V}_2\text{O}_5$  double layer (visible as one faint band between B and D, marked with 2 white lines), (D) substrate of zirconia grains in amorphous  $\text{SiO}_2$ .

for SiV with equivalent vanadia loading. For the TiV particles, selectivities were quite high in both reactions (not shown) [36]. In propane ODH at 823 K, values of around 90% selectivity were observed for all TiV samples (not shown) [21], proving propene to be the primary product.

Despite the equal vanadia dispersion, speciation and degree of polymerisation, an anatase support still yields more active vanadia catalysts than a silica support. The latter illustrates the unique ability of anatase to steer the vanadia film into a layer with superior activity [11]. Conversion of both molecules reaches a maximum for an apparent vanadia surface density of  $\sim 30 \text{ V/nm}^2$  (Fig. 11). On a titania support, such density corresponds to a film of close to 4 theoretical polyvanadate layers, assuming a theoretical polyvanadate monolayer coverage of  $7.5 \text{ V/nm}^2$  [37]. The fact that the support influence is maximal for 4 polyvanadate layers, shows the extent of the anatase–vanadia interaction, reaching well beyond the monolayer. The existence of an active vanadia phase of a few layers thick on anatase, was advanced by other authors, who held it responsible for the enhanced activity [38]. Indeed, in the present case of sputter deposited vanadia films, the anatase support does not influence dispersion or speciation. Hence, the anatase must act through a restructuring of the first vanadia layers into a special phase of up to 4 monolayers thick, yielding an

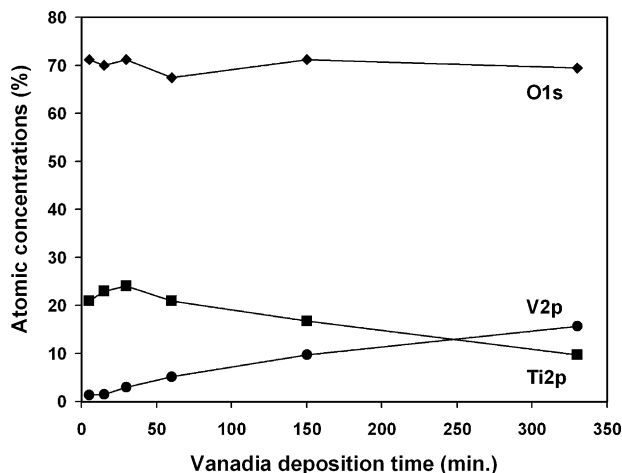


**Fig. 9.** Evolution of O, V and Ti atomic concentrations as a function of vanadia deposition time for vanadia/titania-coated catalysts.

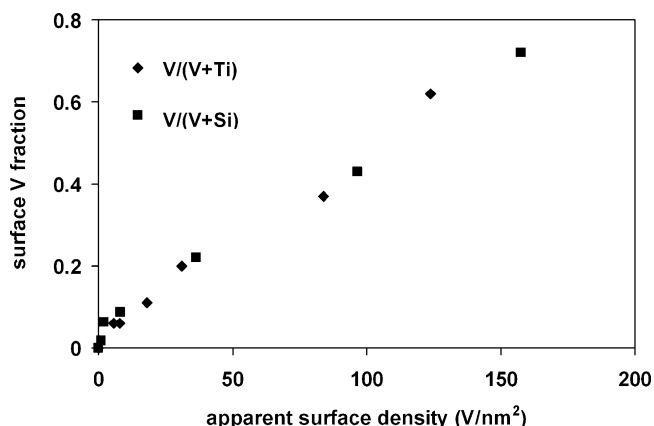


**Fig. 10.** XPS surface fraction of vanadia  $\text{V}/(\text{V} + \text{Ti})$  or  $\text{V}/(\text{V} + \text{Si})$  versus V loading as determined from ICP.

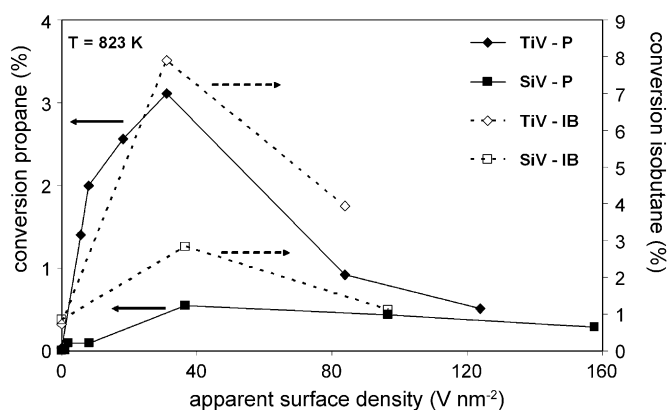


**Fig. 11.** conversions for propane (P) and isobutane (IB) ODH over vanadium oxide thin films supported on silica (SiV) or titania (TiV) versus apparent surface density. Reaction conditions:  $P(\text{C}_3\text{H}_8 \text{ or } \text{iC}_4\text{H}_{10}) = 20 \text{ kPa}$ ,  $P(\text{O}_2) = 10 \text{ kPa}$ ;  $T = 823 \text{ K}$ ; catalyst:  $1.0 \text{ g } (\text{C}_3\text{H}_8)$  and  $0.5 \text{ g } (\text{iC}_4\text{H}_{10})$ ; total flow rate:  $5 \text{ ml min}^{-1} (\text{C}_3\text{H}_8)$  and  $7.5 \text{ ml min}^{-1} (\text{iC}_4\text{H}_{10})$ ; TOS = 300 min.

enhanced activity in ODH of propane and isobutane, rather than by a direct electronic effect through a Ti–O–V bond.

## 5. Conclusions

The deposition of vanadium oxide thin films with physical vapour deposition ensures clean and highly controllable synthesis of model catalysts. The resulting systems are easily accessed with surface sensitive techniques. On flat anatase substrates, XPS–XPD proved that the deposition of a vanadia monolayer was epitaxial, with major crystallographic axes alongside the ones of the underlying anatase. From UPS measurements it followed that fully oxidised thin vanadia depositions could be achieved if the deposition was performed *in situ*. Under influence of photon irradiation, films are slightly photoreduced, resulting in V3p multiplet features and a 3d band developing in the valence band region.

A step closer to industrial supported catalysts was achieved by sputter deposition onto particles in a rotating device. In addition to surface characterisation, these model particle catalysts allow use in reactors for catalytic testing under relevant process conditions. On silica and titania (anatase) supports, thin vanadia films showed similar dispersion, speciation and degree of polymerisation. Hence, sputter deposition allows to eliminate the effect of these 3 properties upon activity, giving the unique opportunity to isolate

the direct support effect. Upon testing the model particles in oxidative dehydrogenation of propane and isobutane, the titania (anatase) support proved superior to silica. Highest activity in alkane ODH appeared for titania supported vanadia thin films of about 4 theoretical monolayers thick. Hence, on titania (anatase), this thin film of vanadia is steered into a special phase showing enhanced activity for ODH reactions with alkanes.

## Acknowledgements

This work was performed in the framework of a Concerted Research Action (GOA-UGent), and of the Belgian Programme on Interuniversity Poles of Attraction (IAP) initiated by the Belgian State, Prime Minister's Office, Science Policy Programming. Geert Silversmit is a Postdoctoral Fellow of the Fund for Scientific Research—Flanders (FWO-Vlaanderen). The scientific responsibility is assumed by its authors.

## References

- [1] H.G. Bachmann, F.R. Ahmed, W.H. Barnes, Z. Krist. 115 (1961) 110.
- [2] J. Haemers, Bull. Soc. Chim. Belges. 79 (1970) 473–478.
- [3] B. Tepper, B. Richter, A.-C. Dupuis, H. Kühlenbeck, C. Hucho, P. Schilbe, M.A. bin Yarmo, H.-J. Freund, Surf. Sci. 496 (2002) 64.
- [4] R.L. Smith, W. Lu, G.S. Rohrer, Surf. Sci. 322 (1995) 293.
- [5] L. Fiermans, J. Vennik, Surf. Sci. 18 (1969) 317.
- [6] A. Da Costa, Chr. Mathieu, Y. Barbaux, H. Poelman, G. Dalmay-Vennik, L. Fiermans, Surf. Sci. 370 (1997) 339.
- [7] G. Silversmit, D. Depla, H. Poelman, G.B. Marin, R. De Gryse, Surf. Sci. 600 (2006) 3512.
- [8] G. Silversmit, D. Depla, H. Poelman, G.B. Marin, R. De Gryse, J. Electr. Spectrosc. 135 (2004) 167.
- [9] B.M. Weckhuysen, D.E. Keller, Catal. Today 78 (2003) 25.
- [10] I.E. Wachs, B.M. Weckhuysen, Appl. Catal. A 157 (1997) 67.
- [11] G.C. Bond, J.C. Védrine, Catal. Today 20 (1994) 1.
- [12] S. Brunauer, P.H. Emmett, E. Teller, J. Am. Chem. Soc. 60 (1938) 309, doi:10.1021/ja01269a023.
- [13] H. Watanabe, K. Itoh, O. Matsumoto, Thin Solid Films 386 (2001) 281.
- [14] J.C. Badot, A. Mantoux, N. Baffier, O. Dubrunfaut, D. Lincot, J. Mater. Chem. 14 (2004) 3411.
- [15] O.R. Nascimento, C.J. Magon, J.F. Lima, J.P. Donoso, E. Benavente, J. Paez, V. Lavayen, M.A. Santa Ana, G. Gonzalez, J. Sol-Gel Sci. Technol. 45 (2008) 195.
- [16] R.T.R. Kumar, B. Karunagaran, V.S. Kumar, Y.L. Jeyachandran, D. Mangalaraj, S.K. Narayandass, Mater. Sci. Semic. Process. 6 (2003) 543.
- [17] W. Gao, C.M. Wang, H.Q. Wang, V.E. Henrich, E.I. Altman, Surf. Sci. 559 (2004) 201.
- [18] C.V. Ramana, R.J. Smith, O.M. Hussain, C.M. Julien, Mater. Sci. Eng. B 111 (2004) 218.
- [19] H. Poelman, H. Tomaszewski, D. Poelman, L. Fiermans, R. De Gryse, M.F. Reyniers, G.B. Marin, Surf. Interface Anal. 34 (2002) 724.
- [20] S. Berg, T. Nyberg, Thin Solid Films 476 (2005) 215.
- [21] H. Poelman, K. Eufinger, D. Depla, D. Poelman, R. De Gryse, B.F. Sels, G.B. Marin, Appl. Catal. A 235 (2007) 213.
- [22] H. Berger, H. Tang, F. Lévy, J. Cryst. Growth 130 (1993) 108.
- [23] H. Sakama, G. Osada, M. Tsukamoto, A. Tanokura, N. Ichikawa, Thin Solid Films 515 (2006) 535.
- [24] W. Gao, E.I. Altman, Surf. Sci. 600 (2006) 2572.
- [25] C.S. Fadley, Prog. Surf. Sci. 16 (1984) 275.
- [26] G. Silversmit, H. Poelman, L. Fiermans, R. De Gryse, Sol. State Comm. 119 (2001) 101.
- [27] H. Poelman, K. Devriendt, L. Fiermans, O. Dewaele, G. Heynderickx, G.F. Froment, Surf. Sci. 377–379 (1997) 819.
- [28] K. Devriendt, H. Poelman, L. Fiermans, Surf. Interface Anal. 29 (2000) 139.
- [29] M. Calatayud, B. Mguig, Chr. Minot, Surf. Sci. 526 (2003) 297.
- [30] H. Poelman, L. Fiermans, J. Vennik, G. Dalmay, Sol. State Commun. 84 (1992) 811.
- [31] G. Silversmit, H. Poelman, D. Depla, D. Poelman, N. Barrett, G.B. Marin, R. De Gryse, Surf. Interface Anal. 38 (2006) 1257.
- [32] R. Zimmermann, R. Claessen, F. Reinert, P. Steiner, S. Hüfner, J. Phys.: Condens. Matter 10 (1998) 5697.
- [33] G. Silversmit, H. Poelman, D. Depla, N. Barrett, G.B. Marin, R. De Gryse, Surf. Sci. 584 (2005) 179.
- [34] H. Poelman, B.F. Sels, M. Olea, K. Eufinger, D. Poelman, J.S. Paul, B. Moens, I. Sack, V. Balcaen, F. Bertinchamps, E.M. Gaigneaux, P.A. Jacobs, G.B. Marin, R. De Gryse, J. Catal. 245 (2007) 156.
- [35] T. Blasco, J.M. López Nieto, Appl. Catal. A 157 (1997) 117.
- [36] M. Olea, I. Sack, V. Balcaen, G.B. Marin, H. Poelman, K. Eufinger, D. Poelman, R. De Gryse, J.S. Paul, B.F. Sels, P.A. Jacobs, Appl. Catal. A 318 (2007) 37.
- [37] A. Khodakov, J. Yang, S. Su, E. Iglesia, A. Bell, J. Catal. 177 (1998) 343.
- [38] G. Centi, Appl. Catal. A 147 (1996) 267.